

Interaction of Four Rarefaction Waves in the Bi-Symmetric Class of the Two-Dimensional Euler Equations

Jiequan Li^{1,*}, Yuxi Zheng^{2,**}

¹ Department of Mathematics, Capital Normal University,
Beijing 100037, Peoples Republic of China

² Department of Mathematics, The Pennsylvania State University,
University Park, PA 16802, USA. E-mail: yzheng@math.psu.edu

Received: 6 August 2008 / Accepted: 27 December 2009
Published online: 24 February 2010 – © Springer-Verlag 2010

Abstract: The global existence and structures of solutions to multi-dimensional unsteady compressible Euler equations are interesting and important open problems. In this paper, we construct global classical solutions to the interaction of four orthogonal planar rarefaction waves with two axes of symmetry for the Euler equations in two space dimensions, in the case where the initial rarefaction waves are large. The bi-symmetric initial data is a basic type of four-wave two-dimensional Riemann problems. The solutions in this case are continuous, bounded and self-similar, and we characterize how large the rarefaction waves must be. We use the methods of hodograph transformation, characteristic decomposition, and phase space analysis. We resolve binary interactions of simple waves in the process.

1. Introduction

Consider the two-dimensional isentropic compressible Euler system

$$\begin{cases} \rho_t + (\rho u)_x + (\rho v)_y = 0, \\ (\rho u)_t + (\rho u^2 + p)_x + (\rho uv)_y = 0, \\ (\rho v)_t + (\rho uv)_x + (\rho v^2 + p)_y = 0, \end{cases} \quad (1.1)$$

where ρ is the density, (u, v) is the velocity and p is the pressure given by $p(\rho) = K\rho^\gamma$, where $K > 0$ will be scaled to be one and $\gamma > 1$ is the gas constant. Cauchy problems for (1.1) are open. Riemann problems for (1.1) are a current research topic, as they are reducible to involve fewer independent variables while retaining important features of general solutions. We refer the reader to [2, 7, 8, 13, 20, 25] for some general solutions to one-dimensional and multidimensional Euler equations, and to [15, 30] for the rich

* Research partially supported by the Key Program from Beijing Educational Commission (KZ200910028002), 973 project (2006CB805902) and PHR(IHLB) and NSFC (10971142).

** Research partially supported by NSF-DMS-0603859, 0908207.

flow patterns displayed by solutions to Riemann problems. Shock reflection problems [5, 19, 24, 31, 34], in particular, are included in the Riemann problems.

Two-dimensional (2-D) Riemann problems are Cauchy problems with special initial data that are constant along each ray from the origin. The one-dimensional case is quite well-understood [4]. The two-dimensional case was formulated, and the solution configurations conjectured, in [28]. The solution configurations are complicated, as confirmed afterward by several numerical simulations [3, 11, 12, 23]. There has been no rigorous proof of the numerical simulations due to lack of effective methods of analysis.

In this paper, with the first success since the proposition [28], we construct analytic solutions to a case of a configuration of the 2-D four-wave Riemann problems of (1.1), using methods that we have developed in recent years. The construction is based on the analysis of (1.1) in three planes: The self-similar variables $(\xi, \eta) = (x/t, y/t)$, the inclination angles of characteristics (α, β) , and the velocity (u, v) -plane of the hodograph transformation. These forms enable us to do analysis effectively.

The case that we solve in this paper has two axes of symmetry. The initial data of a 2-D Riemann problem may possess a certain symmetry, e.g., axial symmetry, or piecewise constant along the axial direction with one or two axes of symmetry of the plane. A global solution for the axially symmetric case has been constructed [29, 33]. Furthermore, a global solution for the binary interaction of two planar rarefaction waves have also been constructed recently [17]. The construction for the interaction of four planar rarefaction waves with one axis of symmetry, a primary class of the two-dimensional four-wave Riemann problems, and denoted as Configuration A in [15, 28, 30], has not been available, but the reason is clearly revealed in paper [10] in which shock formation is established numerically. The shock formation near the sonic boundary makes the global construction difficult. The class of four planar rarefaction waves with two axes of symmetry, which we call bi-symmetric and denote as Configuration B in [15, 28], have also been shown numerically to have shock development in [10] as well as in earlier numerical experiments [3, 12, 15, 23]. However, the extra symmetry makes the configuration accessible by our newly developed tools. We obtain continuous global solutions in this class when the rarefaction waves are large, see Theorem 7.1.

We use the hodograph transformation and characteristic decomposition in constructing the global solution. The characteristic decomposition handles simple waves best while the hodograph transformation, valid for non-simple waves, reduces the system to a linearly degenerate one. Assuming that the flow is ir-rotational and self-similar, Pogodin, Suchkov and Ianenko ([21], 1958) introduced the hodograph transformation to represent the system of equations (1.1) in the velocity variables (u, v) , resulting in a decoupled partial differential equation of second order for the speed of sound c . In 2001, Li ([14]) carried out an analysis of the second order equation in the space (c, u, v) , through a pair of variables resembling the well-known Riemann invariants together with their invariant regions, and established the existence of a solution to the expansion of a wedge of gas into vacuum in the hodograph plane for wide ranges of the gas constant and the wedge angle. In 2006, paper [16] clarified the concept of simple waves for (1.1). Then, in paper [17], we show that the hodograph transformation is non-degenerate (and globally one-to-one) precisely for non-simple waves, and the solutions constructed in [14] in the hodograph plane can be transformed back to the self-similar plane. Thus a complete procedure of construction of solutions is now available, which we use here for studying the interactions involved in Configuration B – the bi-symmetric class. In particular, the interaction of any two simple waves is completed in this paper, provided that the two waves are expanding toward vacuum, see Theorem 6.1.

Our main results are given in Theorems 6.1 and 7.1. A helpful characterization of simple waves, especially their boundaries, is given in Lemma 6.1, which will have broad applications in solving other 2-D Riemann problems. In the next section we list formulas and equations in various forms which form the basis for our construction in this paper. In Sect. 3, we select data to set up Configuration B, eliminating redundancy through scaling and translation or normalization. In Sect. 4, we recall previous work on the interaction of two symmetric planar rarefaction waves. In Sect. 5, we winnow the data to keep the problem hyperbolic. In Sect. 6, we characterize a complete patch of simple wave, as is needed in our solution, and construct the solution of interactions of two simple waves. In Sect. 7, we put the various pieces together to obtain the existence of global solutions, which is stated in Theorem 7.1 and reproduced here:

Theorem (Main theorem). *Consider the Riemann problem for system (1.1) with initial data consisting of constant states (c_i, u_i, v_i) in the i^{th} quadrants ($i = 1, 2, 3, 4$) so that states 1 and 2 form a forward rarefaction wave R_{12}^+ , states 2 and 3 form a backward rarefaction wave R_{23}^- , states 3 and 4 form a forward rarefaction wave R_{34}^+ , and states 4 and 1 form a backward rarefaction wave R_{41}^- . (The rarefaction wave requirement on the data forces $c_2 = c_4, c_1 = c_3$, thus we call it a bi-symmetric problem.) Then, there exists a number $c_2^*(\gamma) \in (0, 1)$ for $\gamma > 1 + \sqrt{2}$, such that our bi-symmetric Riemann problem has global continuous solutions, provided $0 < c_2 < c_2^*(\gamma)c_1$.*

Notations. Here is a list of our notations: Besides the primitive variables $\rho, (u, v)$ and p , we have $c = \sqrt{\gamma p/\rho}$ as the speed of sound, $i = c^2/(\gamma - 1)$ the enthalpy, φ the pseudo-velocity potential. In terms of the self-similar variables (ξ, η) , we often use the pseudo-velocity $(U, V) = (u - \xi, v - \eta)$, and $\Lambda_{\pm}, \lambda_{\pm}$, where

$$\Lambda_{\pm} = \frac{UV \pm c\sqrt{U^2 + V^2 - c^2}}{U^2 - c^2}, \quad \Lambda_{\pm}\lambda_{\mp} = -1. \quad (1.2)$$

The angles α, β and ω are defined as

$$\tan \alpha := \Lambda_+, \quad \tan \beta := \Lambda_-, \quad \omega = (\alpha - \beta)/2, \quad \tau = (\alpha + \beta)/2. \quad (1.3)$$

We also use the following vector fields:

$$\begin{aligned} \partial^{\pm} &= \partial_{\xi} + \Lambda_{\pm}\partial_{\eta}, \quad \partial_{\pm} = \partial_u + \lambda_{\pm}\partial_v, \quad \partial_0 = \partial_u \\ \bar{\partial}^+ &= (\cos \alpha, \sin \alpha) \cdot (\partial_{\xi}, \partial_{\eta}), \quad \bar{\partial}^- = (\cos \beta, \sin \beta) \cdot (\partial_{\xi}, \partial_{\eta}), \quad \bar{\partial}^0 = \cos \tau \partial_{\xi} + \sin \tau \partial_{\eta} \\ \bar{\partial}_+ &= (\sin \beta, -\cos \beta) \cdot (\partial_u, \partial_v), \quad \bar{\partial}_- = (\sin \alpha, -\cos \alpha) \cdot (\partial_u, \partial_v), \end{aligned} \quad (1.4)$$

and some notations

$$\kappa = \frac{\gamma - 1}{2}, \quad m = \frac{3 - \gamma}{\gamma + 1}, \quad \Omega = m - \tan^2 \omega, \quad \tan^2 \theta_s = m, \quad v = \frac{\gamma + 1}{2(\gamma - 1)}. \quad (1.5)$$

2. Systems of Self-Similar Flows

2.1. Irrotational flows. Our primary system is system (1.1) in the self-similar variables $(\xi, \eta) = (x/t, y/t)$:

$$\begin{cases}Ui_{\xi} + Vi_{\eta} + 2\kappa i(u_{\xi} + v_{\eta}) = 0, \\ Uu_{\xi} + Vu_{\eta} + i_{\xi} = 0, \\ Uv_{\xi} + Vv_{\eta} + i_{\eta} = 0\end{cases} \quad (2.1)$$

with the ir-rotationality condition

$$u_\eta = v_\xi. \quad (2.2)$$

System (2.1), (2.2) can also be reduced to the system

$$\begin{cases} (c^2 - U^2)u_\xi - UV(u_\eta + v_\xi) + (c^2 - V^2)v_\eta = 0, \\ u_\eta - v_\xi = 0, \end{cases} \quad (2.3)$$

supplemented by Bernoulli's law

$$i + \frac{1}{2}(U^2 + V^2) = -\varphi, \quad \varphi_\xi = U, \quad \varphi_\eta = V. \quad (2.4)$$

The (pseudo-)characteristics are

$$\Gamma_\pm : \frac{d\eta}{d\xi} = \frac{UV \pm c\sqrt{U^2 + V^2 - c^2}}{U^2 - c^2} \equiv \Lambda_\pm. \quad (2.5)$$

Then system (2.3) can be written in characteristic form:

$$\partial^\pm u + \Lambda_\mp \partial^\pm v = 0. \quad (2.6)$$

2.2. Characteristic decomposition. In [16], it is shown that system (2.3) and (2.4) has a characteristic decomposition, in analogy with that for the classical wave operator. It is very useful in the discussion of simple waves and their interactions.

Proposition 2.1 (Commutator relation). *For any quantity $I(\xi, \eta)$, there holds*

$$\partial^- \partial^+ I - \partial^+ \partial^- I = \frac{\partial^- \Lambda_+ - \partial^+ \Lambda_-}{\Lambda_- - \Lambda_+} (\partial^- I - \partial^+ I). \quad (2.7)$$

Proposition 2.2 (Characteristic decomposition). *For (2.3) and (2.4), there hold*

$$\partial^+ \partial^- I = m_1 \partial^- I, \quad \partial^- \partial^+ J = m_2 \partial^+ J, \quad (2.8)$$

where m_1 and m_2 can be expressed in the form $m_1 = m_1(u, v)(\partial_\xi u + \zeta_1(u, v)\partial_\eta u)$, $m_2 = m_2(u, v)(\partial_\xi u + \zeta_2(u, v)\partial_\eta u)$; and $I = u, v, c$ or Λ_- , $J = u, v, c$ or Λ_+ .

2.3. System in inclination angles of characteristics. The inclination angles (α, β) of characteristics (see notation (1.3)) play an important role in our study. First we have from [17, 32]

$$u - \xi = -c \frac{\cos \tau}{\sin \omega}, \quad v - \eta = -c \frac{\sin \tau}{\sin \omega}. \quad (2.9)$$

System (2.3) can be written as the closed system of equations in terms of α, β , and c :

$$\begin{cases} c\bar{\partial}^-\beta = \Omega \cos^2 \omega (2\sin^2 \omega + c\bar{\partial}^-\alpha), \\ c\bar{\partial}^+\alpha = \Omega \cos^2 \omega [-2\sin^2 \omega + c\bar{\partial}^+\beta], \\ \bar{\partial}^0 c = \frac{\gamma - 1}{2(\gamma + 1)\sin \omega} [4\sin^2 \omega + c\bar{\partial}^-\alpha - c\bar{\partial}^+\beta]. \end{cases} \quad (2.10)$$

Form (2.10) is given in Chen and Zheng [6]. Note that the sign for $\bar{\partial}^0$ here is the opposite of $\bar{\partial}_0$ of [6]. Here we offer a more direct derivation.

Proof of (2.10). We start with the differential relations among the new variables:

$$\begin{aligned} du - d\xi &= -\frac{\cos \tau}{\sin \omega} dc + \frac{c \cos \beta d\alpha - c \cos \alpha d\beta}{2 \sin^2 \omega}, \\ dv - d\eta &= -\frac{\sin \tau}{\sin \omega} dc + \frac{c \sin \beta d\alpha - c \sin \alpha d\beta}{2 \sin^2 \omega}. \end{aligned} \quad (2.11)$$

The differential form of the Bernoulli law (2.4) can be written as

$$dc = \frac{\kappa}{\sin \omega} (\cos \tau du + \sin \tau dv). \quad (2.12)$$

Using (2.6) and (2.11), we have

$$\cot \omega \bar{\partial}^- c = \cos(2\omega) + \frac{c}{2 \sin^2 \omega} [\cos(2\omega) \bar{\partial}^- \alpha - \bar{\partial}^- \beta]. \quad (2.13)$$

The Bernoulli law (2.12) gives

$$\bar{\partial}^- c = \frac{\kappa \sin(2\omega)}{2(\kappa + \sin^2 \omega)} + \frac{c \kappa \cot \omega}{2(\kappa + \sin^2 \omega)} (\bar{\partial}^- \alpha - \bar{\partial}^- \beta). \quad (2.14)$$

The above two equations together give

$$c \bar{\partial}^- \beta = \cos^2 \omega \Omega (2 \sin^2 \omega + c \bar{\partial}^- \alpha). \quad (2.15)$$

Similarly, we have

$$c \bar{\partial}^+ \alpha = \Omega \cos^2 \omega [-2 \sin^2 \omega + c \bar{\partial}^+ \beta]. \quad (2.16)$$

On the other hand, we can obtain the equation for c

$$\begin{aligned} \bar{\partial}^- c &= \frac{\kappa}{1 + \kappa} \cot \omega (2 \sin^2 \omega + c \bar{\partial}^- \alpha), \\ \bar{\partial}^+ c &= -\frac{\kappa}{1 + \kappa} \cot \omega (-2 \sin^2 \omega + c \bar{\partial}^+ \beta). \end{aligned} \quad (2.17)$$

Note that $\cos \omega \bar{\partial}^0 = \frac{\bar{\partial}^+ + \bar{\partial}^-}{2}$. Then we sum up:

$$\bar{\partial}^0 c = \frac{\kappa}{2(1 + \kappa) \sin \omega} [4 \sin^2 \omega + c \bar{\partial}^- \alpha - c \bar{\partial}^+ \beta]. \quad (2.18)$$

Thus we obtain the closed system of equations (2.10). \square

Remark 2.1. In fact, (2.10) can be reduced to a diagonal form,

$$\begin{cases} \bar{\partial}^+(-\beta + \psi(\omega)) = \frac{\sin^2 \omega [\cos(2\omega) - \kappa]}{c(\kappa + \sin^2 \omega)}, \\ \bar{\partial}^-(\alpha + \psi(\omega)) = \frac{\sin^2 \omega [\cos(2\omega) - \kappa]}{c(\kappa + \sin^2 \omega)}, \\ \bar{\partial}^0[c^2(1 + \kappa M^2)] = 2c\kappa M, \end{cases} \quad (2.19)$$

where

$$\psi(\omega) := \sqrt{\frac{\gamma + 1}{\gamma - 1}} \arctan \left(\sqrt{\frac{\gamma - 1}{\gamma + 1}} \cot \omega \right), \quad (2.20)$$

and the pseudo-Mach number M is related to ω as

$$\frac{1}{\sin \omega} = M := \sqrt{U^2 + V^2}/c. \quad (2.21)$$

The Riemann variables $\psi - \beta$ and $\psi + \alpha$ correspond to the classical Riemann invariants for homogeneous systems. However, it is convenient for us to use (2.10) in this paper.

Other useful formulas are given below.

Proposition 2.3. *First-order derivatives have the formulas*

$$\begin{cases} \bar{\partial}_- u = \frac{\sin \alpha}{\kappa} \bar{\partial}_- c, & \bar{\partial}_+ u = -\frac{\sin \beta}{\kappa} \bar{\partial}_+ c, \\ c \bar{\partial}_+ \alpha = -v \Omega \sin(2\omega) \bar{\partial}_+ c, & c \bar{\partial}_- \beta = v \Omega \sin(2\omega) \bar{\partial}_- c, \\ c \bar{\partial}_- \alpha = 2v \tan \omega \bar{\partial}_- c - 2 \sin^2 \omega, & c \bar{\partial}_+ \beta = -2v \tan \omega \bar{\partial}_+ c + 2 \sin^2 \omega, \\ c \bar{\partial}_\pm \omega = (\sin^2 \omega + \kappa) \frac{\tan \omega}{\kappa} \bar{\partial}_\pm c - \sin^2 \omega. \end{cases} \quad (2.22)$$

2.4. System in the hodograph plane. Pogodin, Suchkov and Ianenko [21] proposed the hodograph transformation

$$T : (\xi, \eta) \rightarrow (u, v) \quad (2.23)$$

for (2.1), reversing the roles of (ξ, η) and (u, v) and regarding i as a function of (u, v) . Then i as the function of u and v satisfies

$$\begin{cases} \xi - u = i_u, \\ \eta - v = i_v, \end{cases} \quad (2.24)$$

provided that the transformation (2.23) is non-degenerate. System (2.3) becomes a linearly degenerate system

$$\begin{cases} (2\kappa i(u, v) - i_u^2) \eta_v + i_u i_v (\xi_v + \eta_u) + (2\kappa i - i_v^2) \xi_u = 0, \\ \xi_v - \eta_u = 0 \end{cases} \quad (2.25)$$

for the unknowns (ξ, η) . And i satisfies

$$(2\kappa i - i_u^2) i_{vv} + 2i_u i_v i_{uv} + (2\kappa i - i_v^2) i_{uu} = i_u^2 + i_v^2 - 4\kappa i. \quad (2.26)$$

The linear degeneracy of (2.25) becomes more transparent when it is expressed in terms of α, β and c . In paper [17], we convert (2.26) to

$$\begin{cases} \bar{\partial}_+ \alpha = \frac{1+\gamma}{4c} \cdot \sin(\alpha - \beta) \cdot [m - \tan^2 \omega] =: G(\alpha, \beta, c), \\ \bar{\partial}_- \beta = G(\alpha, \beta, c), \\ \partial_0 c = \kappa \cos \frac{\alpha+\beta}{2} / \sin \omega, \end{cases} \quad (2.27)$$

with

$$\bar{\partial}_+ c = -\kappa, \quad \bar{\partial}_- c = \kappa. \quad (2.28)$$

The definitions of $\bar{\partial}_\pm$ and ∂_0 (see (1.4)) implies that system (2.27) is linearly degenerate.

In our construction of solutions, we need C^0 , C^1 and $C^{1,1}$ estimates. The main difficulty lies in the non-homogeneity of (2.27). Thus we shall need the second-order derivatives, given in [17], which are obtained by direct calculation.

Proposition 2.4. Assume that the solution of (2.27) $(\alpha, \beta) \in C^2$. Then we have

$$\begin{cases} \bar{\partial}_+ \bar{\partial}_- \alpha + W \bar{\partial}_- \alpha = Q(\omega, c), \\ -\bar{\partial}_- \bar{\partial}_+ \beta + W \bar{\partial}_+ \beta = Q(\omega, c), \end{cases} \quad (2.29)$$

where $W(\omega, c)$ and $Q(\omega, c)$ are

$$\begin{aligned} W(\omega, c) &:= \frac{1+\gamma}{4c} \left[(m - \tan^2 \omega) (3 \tan^2 \omega - 1) \cos^2 \omega + 2 \tan^2 \omega \right], \\ Q(\omega, c) &:= \frac{(1+\gamma)^2}{16c^2} \sin(2\omega) (m - \tan^2 \omega) (3 \tan^2 \omega - 1). \end{aligned} \quad (2.30)$$

Proposition 2.5. Assume that the solution of (2.27) $(\alpha, \beta) \in C^2$. Then we have

$$\begin{cases} \bar{\partial}_+ \bar{\partial}_- (\alpha + \beta) + W \bar{\partial}_- (\alpha + \beta) = a(\omega, c) \bar{\partial}_+ (\alpha + \beta) \\ -\bar{\partial}_- \bar{\partial}_+ (\alpha + \beta) + W \bar{\partial}_+ (\alpha + \beta) = a(\omega, c) \bar{\partial}_- (\alpha + \beta), \end{cases} \quad (2.31)$$

where

$$a(\omega, c) := \frac{\gamma+1}{4c} \cos^2 \omega (\tan^2 \omega + \alpha_2) (\tan^2 \omega - \alpha_1), \quad (2.32)$$

where

$$\alpha_2 := \frac{1}{2} [3 + m + \sqrt{(3+m)^2 + 4m}], \quad \alpha_1 := \frac{2m}{3 + m + \sqrt{(3+m)^2 + 4m}}. \quad (2.33)$$

Proposition 2.6. Assume that the solution of (2.27) $(\alpha, \beta) \in C^2$. Then we have

$$\begin{cases} (\bar{\partial}_+ + W)(Z - \bar{\partial}_- \alpha) = \frac{\gamma+1}{4c} (\tan^2 \omega + 1) (Z - \bar{\partial}_+ \beta) \\ (-\bar{\partial}_- + W)(Z - \bar{\partial}_+ \beta) = \frac{\gamma+1}{4c} (\tan^2 \omega + 1) (Z - \bar{\partial}_- \alpha), \end{cases} \quad (2.34)$$

where

$$Z := \frac{\gamma+1}{2c} \tan \omega. \quad (2.35)$$

To invert the solution on the hodograph plane to the (ξ, η) plane, we notice that (2.24) defines a mapping from (u, v) to (ξ, η) as $\xi = u + i_u$, $\eta = v + i_v$. The Jacobian has the formula

$$j(\xi, \eta; u, v) = \frac{\partial(\xi, \eta)}{\partial(u, v)} = \frac{c^2}{4 \sin^4 \omega} (\bar{\partial}_- \alpha - Z)(\bar{\partial}_+ \beta - Z). \quad (2.36)$$

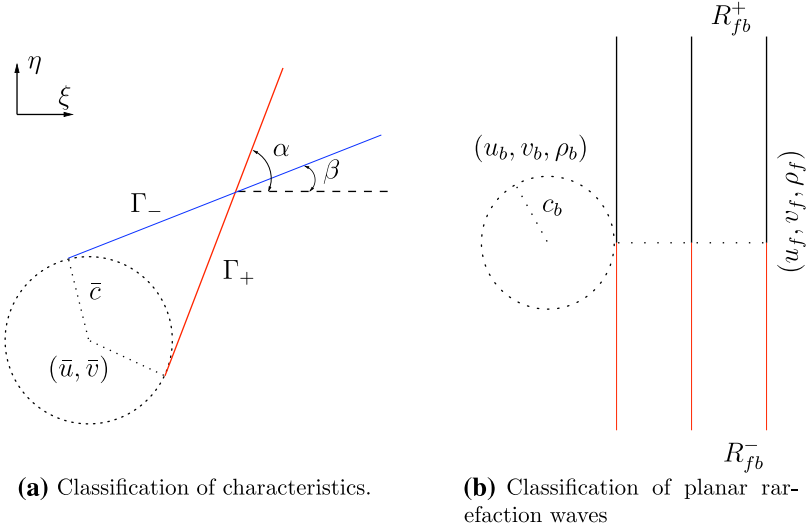


Fig. 3.1. Illustration of characteristics and planar rarefaction waves

3. Bi-symmetric Four Rarefaction Waves

The initial data for the 2-D Riemann problem are constant along each ray from the origin,

$$(u, v, \rho)(t, x, y)|_{t=0} = (u_0, v_0, \rho_0)(\theta), \quad \theta = \arctan(y/x). \quad (3.1)$$

For theoretical and application reasons, $(u_0, v_0, \rho_0)(\theta)$ is usually piecewise constant. The four-constant Riemann problem is a prototype example and has special initial data that takes on constant values in each of the four initial quadrants; i.e.,

$$(u_0, v_0, \rho_0)(\theta) = (u_i, v_i, \rho_i), \quad (i-1)\pi/2 < \theta < i\pi/2, \quad (3.2)$$

($i = 1, 2, 3, 4$). We use I, II, III and IV to designate the corresponding state (u_i, v_i, ρ_i) . The four-wave Riemann problem is restricted further so that each adjacent pair of data in the four-constant Riemann problem is connectible by a single planar wave. See [28].

The characteristics defined by (2.5) in the region of a constant state provide a basic reference point for understanding non-constant states. The characteristics are straight lines and the set $\{(\xi, \eta); (\xi - \bar{u})^2 + (\eta - \bar{v})^2 = \bar{c}^2\}$ is a *sonic circle* of the state $(\bar{u}, \bar{v}, \bar{\rho})$. The plus characteristic lines, denoted by Γ_+ in Fig. 3.1(a), are tangent to the sonic circle, and go in the counterclockwise direction if regarded as starting at the tangent points in reference to the sonic circle, while Γ_- go clockwise.

The Euler system (1.1) has two classes of planar rarefaction waves connecting a given pair of states (u_f, v_f, ρ_f) and (u_b, v_b, ρ_b) . We denote the first class by R_{fb}^+ , whose tell-tale feature is that the family of straight-line characteristics go *counter-clockwise* in reference to the sonic circle of the state (u_b, v_b, ρ_b) . We denote the second class by R_{fb}^- , whose tell-tale feature is that the family of straight-line characteristics go *clockwise* in reference to the sonic circle of the state (u_b, v_b, ρ_b) . The two classes have examples represented by

$$R_{fb}^\pm : \begin{cases} \xi = u + c, \quad \frac{du}{d\rho} = \frac{c}{\rho}, \quad v = v_f = v_b, \quad \rho_b < \rho_f \\ \eta > v_b \text{ or } \eta < v_b. \end{cases} \quad (3.3)$$

We designate that the front is the state with higher pressure, or equivalently, higher density, as shown in Fig. 3.1(b).

We require our initial data (3.2) to have R_{12}^+ connecting states I and II, R_{14}^- connecting states I and IV, R_{32}^- connecting states III and II, and R_{34}^+ connecting states III and IV. These requirements place strong restrictions on the four states and a number of compatibility conditions result. In the end, see [15], however, we only need

$$\rho_1 = \rho_3, \quad \rho_2 = \rho_4, \quad u_1 - u_2 = v_1 - v_4 \quad (\rho_2 < \rho_1). \quad (3.4)$$

And the set-up is symmetric with respect to

$$\xi - \eta = u_1 - v_1 \quad \text{and} \quad \xi + \eta = u_2 + v_2.$$

So our data enjoys two axes of symmetry and so we call it bi-symmetric data. It is denoted traditionally **Configuration B** $R_{12}^+ R_{14}^- R_{32}^- R_{34}^+$, see [12, 15, 22, 23, 28, 30].

In a recent paper [17] we handled the interaction of an R^+ with an R^- at any angle between 0 and π . It is a fundamental case of wave interactions. We use it in this paper to consider the bi-symmetric configuration, where the interaction of $R_{12}^+ R_{14}^-$ is to interact with the interaction of $R_{32}^- R_{34}^+$, which is really the second level interaction of primary binary interactions, cf. Dinu [9].

Normalization. We use scaling and translations to get rid of unnecessary freedom in the data to prepare for our construction. We note that ξ and u can be shifted by an equal amount without changing the solution. The same is true for η and v . So we shall assume that

$$u_1 - v_1 = 0, \quad u_2 + v_2 = 0. \quad (3.5)$$

In addition, the transformation $(u, v, c, \xi, \eta) \rightarrow \bar{c}(u, v, c, \xi, \eta)$ (where \bar{c} is any positive constant) does not change system (2.1), so we shall assume that

$$c_1 = 1. \quad (3.6)$$

Thus we have only two free parameters: $c_2 \in (0, 1)$ and $\gamma > 1$. And there hold

$$u_1 = \frac{c_1 - c_2}{\gamma - 1} > 0, \quad v_1 = v_2 = u_1, \quad u_2 = -u_1. \quad (3.7)$$

The rarefaction wave R_{12}^+ has the explicit expression

$$\begin{aligned} \xi &= u_1 + \int_{\rho_1}^{\rho} \rho^{-1} \sqrt{p'(\rho)} d\rho + \sqrt{p'(\rho)}, \quad \rho_2 < \rho < \rho_1, \\ v &= v_1, \\ u &= u_1 + \int_{\rho_1}^{\rho} \rho^{-1} \sqrt{p'(\rho)} d\rho, \\ \eta &> v_1. \end{aligned} \quad (3.8)$$

The characteristics of the plus family are straight lines; the characteristics of the minus family are given by

$$\eta = v_1 + \rho^{\frac{\gamma+1}{4}} \sqrt{\bar{c} + \frac{\gamma(\gamma+1)}{3-\gamma} \rho^{\frac{\gamma-3}{2}}}, \quad (3.9)$$

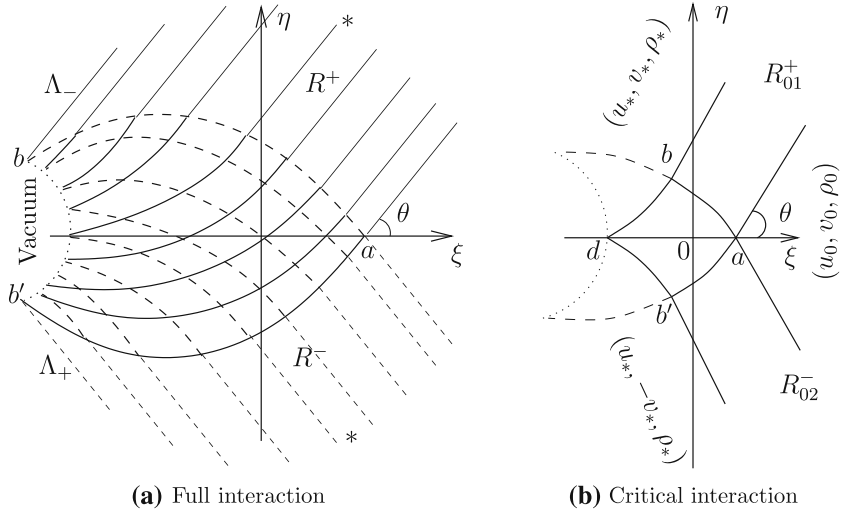


Fig. 4.1. Interaction of planar rarefaction waves: In (a) we show the case of gas expansion into a vacuum; In (b) we show the critical case that the vacuum interface is a single point

where \bar{c} is a constant, for $\gamma \neq 3$. For $\gamma = 3$, the characteristics are

$$\eta = v_1 + \rho \sqrt{\bar{c} - 6 \ln \rho}. \quad (3.10)$$

For the special minus characteristic curve that starts horizontally (i.e., the curve ab in Fig. 5.1) we have

$$\bar{c} = -\frac{2\gamma(\gamma-1)}{3-\gamma} \rho_1^{\frac{\gamma-3}{2}} \quad (3.11)$$

for $\gamma \neq 3$, and

$$\bar{c} = 3 + 6 \ln \rho_1 \quad (3.12)$$

for $\gamma = 3$.

4. Binary Interaction of Planar Rarefaction Waves

Before constructing the global solution for the four bi-symmetric rarefaction waves we proposed last section, we recall the binary interaction of planar rarefaction waves from [17]. The most typical case is the interaction of full rarefaction waves R^+ and R^- that connect the vacuum to a constant state, as shown in Fig. 4.1(a). These two waves penetrate each other completely and fully expand into the vacuum.

Lemma 4.1 (Gas expansion [17]). *There exists a solution $(u, v, \rho) \in C^1$ of (1.1) for the problem of gas expansion into a vacuum in the wave interaction region in the self-similar (ξ, η) -plane for all $\gamma \geq 1$ and all wedge half-angle $\theta \in (0, \pi/2]$. For $\theta > \theta_s := \arctan(Re \sqrt{\frac{3-\gamma}{\gamma+1}})$, the vacuum boundary is representable as a single-valued concave function $\xi = B(\eta)$, the minus family of characteristics are concave, the plus family of characteristics are convex, and the difference of their inclination angles at the boundary is $2\theta_s(\gamma)$.*

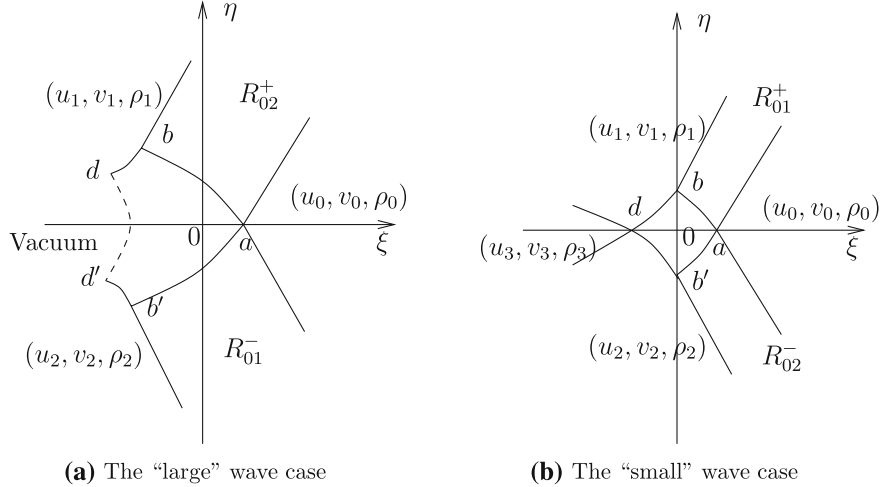


Fig. 4.2. Interaction of two symmetric rarefaction waves: In (a) the data satisfies $0 \leq \rho_1 = \rho_2 < \rho_* < \rho_0$; In (b) the data satisfies $\rho_* \leq \rho_1 = \rho_2 < \rho_0$

As a corollary, we can study the interaction of two planar rarefaction waves R_{01}^+ and R_{02}^- in Fig. 4.1(b), R_{01}^+ connecting states (u_0, v_0, ρ_0) and (u_1, v_1, ρ_1) , R_{02}^- connecting states (u_0, v_0, ρ_0) and (u_2, v_2, ρ_2) , for two appropriate states (u_1, v_1, ρ_1) and (u_2, v_2, ρ_2) . These two waves penetrate each other. Here we state a symmetric case: $u_1 = u_2$, $v_1 = -v_2$ and $\rho_1 = \rho_2$, and fix the state (u_0, v_0, ρ_0) . Then it is evident that there exists a state (u_*, v_*, ρ_*) such that if $(u_1, v_1, \rho_1) = (u_*, v_*, \rho_*)$ and $(u_2, v_2, \rho_2) = (u_*, -v_*, \rho_*)$, the vacuum interface just shrinks into a single point. That is, the wave-tail characteristics from points b and b' meet at a point d at which the density is zero. This case is referred to as the critical case.

Once the states (u_1, v_1, ρ_1) and (u_2, v_2, ρ_2) are such that $\rho_1 = \rho_2 < \rho_*$, then the vacuum interface is no longer a single point. We refer to this case as the “large” rarefaction waves.

We summarize the interaction of planar rarefaction waves in the following corollary.

Corollary 4.1. *For the interaction of two symmetric planar rarefaction waves R_{01}^+ and R_{02}^- , there are three cases of solutions. For the large data case, they expand into vacuum and an interface separates the vacuum from the interaction region; For the small data case, they penetrate each other without the presence of vacuum. The third case is the middle case when the data yields a single point of vacuum. See Fig. 4.2.*

We remark that we do not have any quantitative estimate on the location of the vacuum boundary $\xi = B(\eta)$, e.g., the value of $B(0)$.

5. Hyperbolicity and Non-overlapping of Domains of Determinacy

We start the construction of solutions. See Fig. 5.1. The interaction of $R_{12}^+ R_{14}^-$ follows from Lemma 4.1 and Corollary 4.1. So does the interaction of $R_{32}^- R_{34}^+$. Under our normalization, the interaction point a has the coordinate

$$a = (\xi_1, \eta_1) = \left(\frac{1 - c_2}{\gamma - 1} + 1, \quad \frac{1 - c_2}{\gamma - 1} + 1 \right),$$

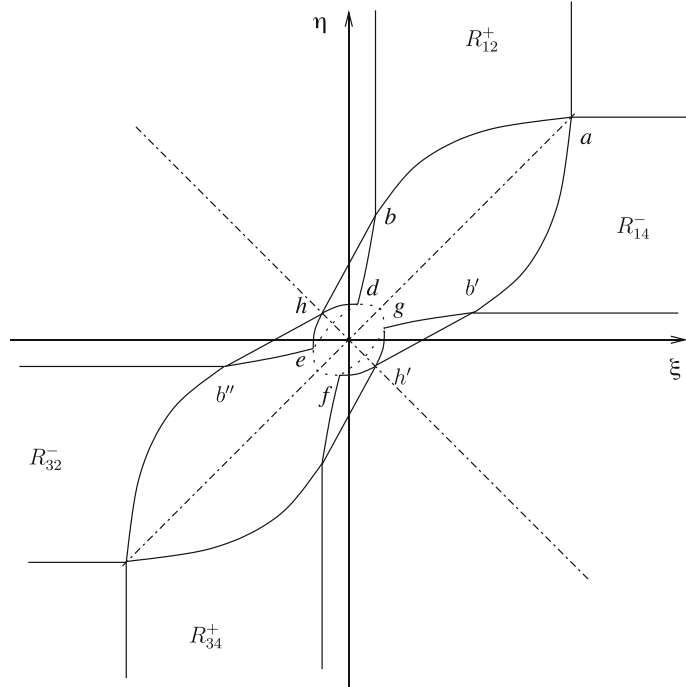


Fig. 5.1. Interaction of four bi-symmetric rarefaction waves

which follows from (3.6), (3.7) and the solution formula $\xi = u + c$ for R_{12}^+ . Similarly, point b has the horizontal coordinate

$$\xi_b = u_2 + c_2 = -\frac{1 - c_2}{\gamma - 1} + c_2 = -\frac{1}{\gamma - 1} + \frac{\gamma c_2}{\gamma - 1}.$$

Depending on the magnitude c_2 of state II, we may or may not have a portion of the sonic circle of state II in the solution. We require that state II has no sonic point. In other words, the characteristic lines bh and $b''h$ intersect before contacting the sonic circle of state II. Thus we need the exiting slope of the minus characteristic curve (line bh), that starts horizontally from the first quadrant, to be greater than one, so that it will intersect its counterpart (line $b''h$) from the interaction of $R_{32}^-R_{34}^+$ before hitting the sonic circle of state II.

Lemma 5.1. *For state II to be hyperbolic at point h it is necessary and sufficient to have $\gamma > 1 + \sqrt{2}$ with*

$$\rho_2/\rho_1 < \left[\frac{(2 - \sqrt{2})(\gamma - 1)}{2(\gamma - 1 - \sqrt{2})} \right]^{\frac{2}{\gamma-3}} \quad (5.1)$$

for $\gamma \neq 3$, and

$$\rho_2/\rho_1 < \exp(-\sqrt{2} - 1) \quad (5.2)$$

for $\gamma = 3$.

Proof. For $\gamma = 3$, we have $c = \sqrt{p'} = \sqrt{3}\rho$, $u = c + u_1 - c_1$, $\xi = u + c = u_1 - c_1 + 2\sqrt{3}\rho$ in R_{12}^+ . The characteristic curve ab is given by (3.10) with data (3.12) or

$$\eta = v_1 + \rho \sqrt{3 + 6 \ln(\rho_1/\rho)}. \quad (5.3)$$

We then compute

$$\frac{d\eta}{d\xi} = \frac{d\eta/d\rho}{d\xi/d\rho} = \frac{\ln(\rho_1/\rho)}{\sqrt{1 + 2 \ln(\rho_1/\rho)}}. \quad (5.4)$$

Requiring the slope to be greater or equal to one, we find

$$\rho_1/\rho \geq e^{\sqrt{2}+1}. \quad (5.5)$$

Next for $\gamma \neq 3$, we use ξ from (3.8) and η from (3.9) with data (3.11) to compute

$$\frac{d\xi}{d\rho} = \frac{\gamma+1}{2} \sqrt{\gamma} \rho^{\frac{\gamma-3}{2}}; \quad \frac{d\eta}{d\rho} = \frac{\gamma(\gamma+1)(\gamma-1)}{2(3-\gamma)(\eta-v_1)} \rho^{\frac{\gamma-1}{2}} (\rho^{\frac{\gamma-3}{2}} - \rho_1^{\frac{\gamma-3}{2}}). \quad (5.6)$$

We require that the slope be greater or equal to one, i.e., $d\eta/d\xi \geq 1$ which simplifies to

$$\frac{\gamma-1}{\sqrt{\gamma+1}} \frac{1}{\sqrt{x}} \frac{x-1}{3-\gamma} \geq \sqrt{\frac{1}{\gamma+1} + \frac{x-1}{3-\gamma}} \quad (5.7)$$

for

$$x := (\rho/\rho_1)^{\frac{\gamma-3}{2}}.$$

We then factorize (5.7),

$$(\gamma^2 - 2\gamma - 1) \left[x - \frac{(2 + \sqrt{2})(\gamma - 1)}{2(\gamma + \sqrt{2} - 1)} \right] \left[x - \frac{(2 - \sqrt{2})(\gamma - 1)}{2(\gamma - \sqrt{2} - 1)} \right] \geq 0, \quad (5.8)$$

which then reduces to our conclusion. This completes the proof. \square

Non-overlapping of domains of determinacy. In addition to a hyperbolic point h , we shall choose c_2 lower enough so that the point d is a vacuum. We do not have a quantity of c_2 to tell when this happens — its value is most probably a numerical one, depending on γ only, under the current normalization (3.5), (3.6). The reason that we require d to be a vacuum is to minimize further interaction.

Further, we need point d to be above the line $\xi + \eta > 0$; i.e., $\xi_d > -\eta_d$, which may require R_{12}^+ to be possibly larger than before. We need it because we want to avoid overlapping of the domains of determinacy of the interactions $R_{12}^+ R_{14}^-$ and $R_{32}^- R_{34}^+$. We explain that this is achievable. In fact, it is sufficient to require that

$$\beta > \pi/4 \quad (5.9)$$

along the plus characteristic curve db in Fig. 5.1. We use Fig. 5.2 for better illustration, in which the curve ab has a tangent line at point b with an inclination angle greater than $\pi/4$. Note that the lines to the left of curve $c_2 bd$ are not present in the four-rarefaction wave interaction because they are shadowed by the state $c_2 > 0$, except for the segment bh . Since the curve abb_0 is concave, we see that the value of β at b_0 is also greater than $\pi/4$.

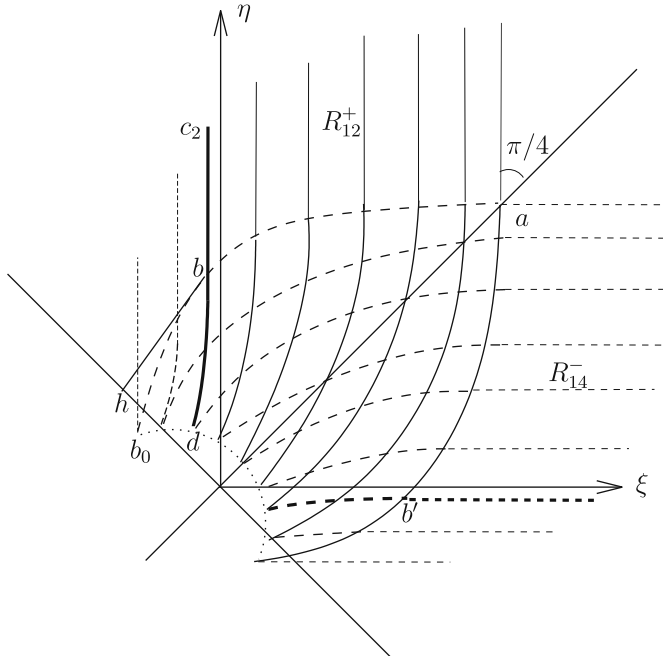


Fig. 5.2. Interaction of two rarefaction waves in rotated coordinate

Using the fact that the solution to the binary interaction is continuous, we see that β on the curve bd will be greater than $\pi/4$ once the point b is sufficiently close to point b_0 . We call such a critical value of c_2 (so that $\beta \geq \pi/4$ along curve bd) c_2^0 . That is,

$$c_2^0 = \sup\{c_2 \in (0, 1) \mid \beta > \pi/4 \text{ on plus characteristic curve } bd\}. \quad (5.10)$$

We explain now that condition (5.9) implies point d is above the line $\xi + \eta = 0$. Let us rotate the coordinate system of Fig. 5.2 counter-clockwise by $\pi/4$, so that we regard the line $\xi - \eta = 0$ as the new ξ -axis, called $\tilde{\xi}$ -axis. In rotated Fig. 5.2, we note that the velocity component along the $\tilde{\xi}$ -axis is

$$\tilde{u} = (u + v)/\sqrt{2}.$$

In particular we have $\tilde{u} = 0$ at point b due to our normalization $u_2 + v_2 = 0$. We observe that

$$\bar{\partial}^+ \tilde{u} = -\frac{\sin \tilde{\beta}}{\kappa} \bar{\partial}^+ c$$

holds along db , which we can integrate to find that $\tilde{u} > 0$ at point d , since $\tilde{\beta} > 0$ along db and c is increasing from d to b . We observe further that $\tilde{\xi} \geq \tilde{u}$ at the vacuum from $\xi - u = c \frac{\cos \tau}{\sin \omega} \geq 0$, thus $\xi + \eta = \sqrt{2}\tilde{\xi} > 0$ at point d . In sum,

Proposition 5.1. Suppose $c_2 \in (0, c_2^0)$. Then we have $\beta > \pi/4$ along curve bd , point h is hyperbolic and point d is above the line $\xi + \eta = 0$.

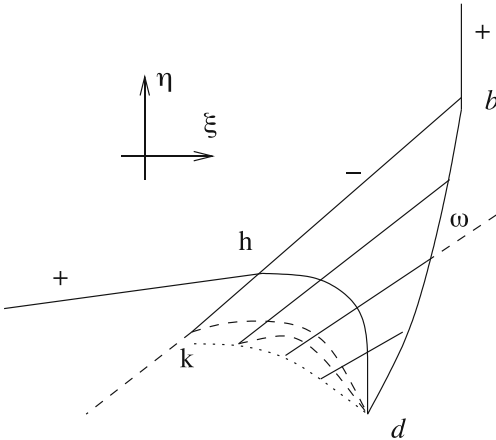


Fig. 6.1. A patch of simple wave

6. Simple Waves and Their Interaction

6.1. A complete patch of simple wave. In [16] we showed that adjacent to a constant state is a simple wave, by using the characteristic decomposition (2.2). Thus the region adjacent to state II and covered by the curvilinear boundaries bhd in Fig. 5.1 is a simple wave. We show that its vacuum boundary is the single point d , and the boundary hd is a characteristic curve of the plus family. See Fig. 6.1.

Lemma 6.1 (Simple wave). *Let bd be a characteristic curve of the plus family, along which the density ρ decreases from point b to zero at point d . Let bk be a straight characteristic curve, where point k is sonic. Then a simple wave exists, forming a curvilinear triangle bkd , for which the boundary kd (the dotted curve in Fig. 6.1) is sonic, and each of the characteristics of the plus family extends from point d to a point on bk or kd .*

Remark. We do not know if β is monotone along the curve bd .

Proof. It follows from [16] that the patch is a simple wave, in which the characteristics of the minus family are straight lines, along which the density is constant. Thus point k is a sonic point where $U^2 + V^2 - c^2 = 0$. Every minus characteristic ends at a sonic point instead of vacuum. The length of the minus characteristics inside the patch shrinks to zero since the density shrinks to zero. The minus characteristics do not form shocks inside the patch since it can be shown, following the idea and proofs of [1, 18, 26], that the $\bar{\partial}^+ c$ is always finite. In fact, we claim that

$$-\bar{\partial}^- (\bar{\partial}^+ c) = \frac{1}{2c} \left[2 \sin(2\omega) - \frac{1+\kappa}{\kappa \cos^2 \omega} \bar{\partial}^+ c \right] \bar{\partial}^+ c. \quad (6.1)$$

We derive (6.1) as follows. We use $I = c$ in the commutator relation (2.7) and $\partial^- c = 0$ to obtain

$$\partial^- \partial^+ c = \frac{\partial^- \tan \alpha - \partial^+ \tan \beta}{\tan \beta - \tan \alpha} (-\partial^+ c).$$

We use $\partial^- \beta = 0$ in (2.10) to obtain

$$2 \sin^2 \omega + c \bar{\partial}^- \alpha = 0. \quad (6.2)$$

So we obtain

$$\partial^- \tan \alpha = \frac{1}{\cos^2 \alpha} \partial^- \alpha = -\frac{2 \sin^2 \omega}{c \cos \beta \cos^2 \alpha}.$$

We use (2.17) to obtain

$$\partial^+ \tan \beta = \frac{1}{c \cos^2 \beta \cos \alpha} c \bar{\partial}^+ \beta = \frac{1}{c \cos^2 \beta \cos \alpha} \left[2 \sin^2 \omega - \frac{1+\kappa}{\kappa} \tan \omega \bar{\partial}^+ c \right].$$

In addition, we have

$$\bar{\partial}^- \bar{\partial}^+ c = \cos \beta [\partial^- (\cos \alpha \bar{\partial}^+ c)] = \cos \alpha \cos \beta \partial^- \bar{\partial}^+ c - \tan \alpha \bar{\partial}^- \alpha \bar{\partial}^+ c.$$

Using (6.2) again, we obtain

$$\bar{\partial}^- \bar{\partial}^+ c = \cos \alpha \cos \beta \partial^- \bar{\partial}^+ c + 2c^{-1} \sin^2 \omega \tan \alpha \bar{\partial}^+ c.$$

Combining the above and using $\cos \alpha + \cos \beta = 2 \cos \tau \cos \omega$ and $\sin \omega \sin \alpha - \cos \tau = -\cos \alpha \cos \omega$, we obtain (6.1).

In (6.1), the direction $\bar{\partial}^+$ is going from d to b , thus $\bar{\partial}^+ c > 0$ on the curve db . The direction of $-\bar{\partial}^-$ is going from b to h . Because the right-hand side has the factor $\bar{\partial}^+ c$, it does not get to zero. And because the coefficient of the quadratic term is negative, it does not grow to positive infinity. Thus $\bar{\partial}^+ c > 0$ remain positive and finite in the whole patch of the simple wave. This proves the above claim.

We need to show that the plus characteristics do not start from an interior point of the boundary kd . From (6.2), we obtain that along a minus characteristic,

$$\sin^2 \omega + c \bar{\partial}^- \omega = 0, \quad (6.3)$$

thus ω is monotone increasing in the direction parallel to that from b to k . Following the monotonicity, we can conclude that the plus characteristics cannot start from an interior point of the boundary kd . Because, if it does, then ω would be zero at the starting point, but our ω on the “initial” line bd is positive, thus contradicting the monotonicity along the minus characteristics connecting the starting point and the initial point on bd . This completes the proof of the lemma. \square

6.2. Interaction of simple waves. We consider the interaction of two simple waves. The two simple waves will be quite general, with quite general interaction angles, which will include the interaction of the waves bhd with $b''he$, as well as the interaction of R_{12}^+ with R_{14}^- , see Fig. 5.1.

Let us take a survey on what angles of interactions are involved in our bi-symmetric interaction. The interaction half-angle of R_{12}^+ with R_{14}^- is $\pi/4$. For the interaction at point h , the maximum angle $\pi/2$ is achieved when bh is parallel to $b''h$, while the minimum angle $\pi/4$ is achieved when the point h becomes vacuum so that bh becomes bd and thus bh is perpendicular to $b''h$. Therefore we shall need interaction (half-)angles between $(\pi/4, \pi/2)$.

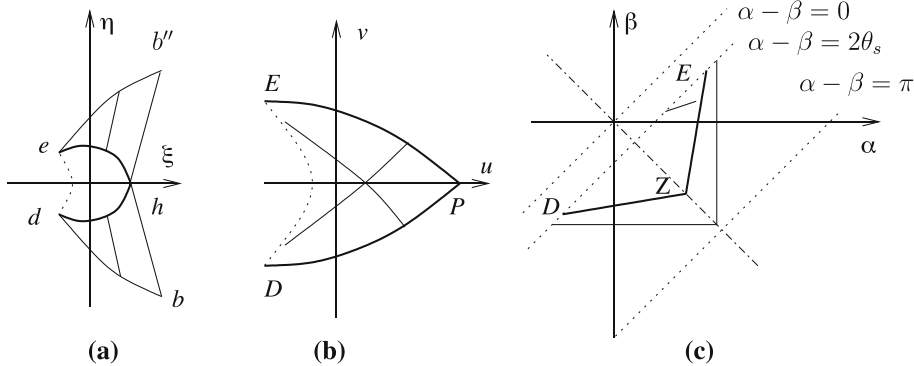


Fig. 6.2. Interaction of two simple waves

We use the interaction bhd with $b''he$ as the primary problem and $\gamma > 1 + \sqrt{2}$. Notice that the Suchkov angle $\theta_s(\gamma)$ is less than $\pi/4$ for $\gamma > 1$, so our interaction half-angles are always greater than the Suchkov angles, hence our interactions belong to the large angle case following the terminology of paper [17].

Thus we consider data as shown in Fig. 6.2, part (a). The data is symmetric with respect to the ξ -axis. Point h is on the ξ -axis. The lower curvilinear triangle bhd is a simple wave in which bh is a straight characteristic curve of the minus family, while d is vacuum. The density is monotone decreasing to zero from h to d along hd , and hd is a convex characteristic curve of the plus family. Length of hd is finite. We need to construct the interaction zone dhe , where the dotted curve de is vacuum.

Part (b) of Fig. 6.2 represents the hodograph domain of interaction, while part (c) of Fig. 6.2 represents the phase space (α, β) , where the three lower branches of parts (a), (b), and (c) represent the same boundary.

Local existence of the solution at point P in part (b) of Fig. 6.2 follows from the standard argument for Goursat problems, see [27, 32] for example. We need uniform estimates on (α, β) and their derivatives to extend the local solution up to the vacuum boundary.

Curve DZ in part (c) of Fig. 6.2 represents the relation between α and β on the boundary dh of part (a) of Fig. 6.2. It is a horizontal straight segment if the simple wave bhd is a planar wave. We note, once we require condition (5.10) that $c_2 < c_2^0$, that $\beta > -\pi/2$ along DZ , i.e., the slopes of the straight lines in curvilinear triangle bhd of part (a) of Fig. 6.2 is negative but not $-\infty$. Similarly, we have $\alpha < \pi/2$ along the boundary EZ in part (c) of Fig. 6.2. Thus we can use

$$\beta = \min_{DZ} \beta, \quad \alpha = \max_{EZ} \alpha \quad (6.4)$$

to form the bottom and right sides of an invariant triangle for (α, β) , while the third side is the line $\alpha - \beta = 2\theta_s$ for $\gamma \in (1 + \sqrt{2}, 3)$ or $\alpha - \beta = 0$ for $\gamma \geq 3$. The fact that the three straight-lines are not penetrable has been established in paper [17]. Hence the (α, β) are bounded in this way:

$$\alpha \leq \max_{EZ} \alpha, \quad \beta \geq \min_{DZ} \beta, \quad \alpha - \beta \geq 2\theta_s(\gamma), \quad (6.5)$$

where we use $\theta_s(\gamma) = 0$ for $\gamma \geq 3$.

Now that the invariant region (6.5) for (α, β) is available, the derivatives of (α, β) can be shown to be bounded in terms of $c > 0$, see [17, 32]. We omit the details. Thus, a global solution exists where $c > 0$ in region DPE .

Using Proposition 2.6, we can invert the mapping to yield a solution in the $\xi - \eta$ plane. By the invariance of the (α, β) of (6.5), we obtain that the characteristics in the $\xi - \eta$ plane are either convex or concave. We summarize this subsection in a theorem.

Theorem 6.1 (Simple wave interactions). *Interaction of two simple waves with an interaction half-angle between $(\pi/4, \pi/2)$ and a density vanishes along the interaction boundaries exists as a smooth solution, in which the plus family of characteristics are convex while the minus family is concave, provided that $c_2 \in (0, c_2^0)$.*

7. Global Solution

We construct the global solution for the bi-symmetric four rarefaction wave interaction. The first interaction of R_{12}^+ with R_{14}^- has been done in [17], and it also follows from the previous section, for any $c_2 \in [0, 1]$. We need the wave R_{12}^+ to be large, by choosing c_2 close to zero, so that the point d of Fig. 5.1 is a vacuum and point h is hyperbolic. Choosing $c_2 \in (0, c_2^0)$, we avoid point d running into point e and obtain the global existence of the interaction of the two simple waves dhe at the same time. We summarize our results in a theorem.

Theorem 7.1 (Global existence). *Suppose $\gamma > 1 + \sqrt{2}$. Then there exists $c_2^0(\gamma) \in (0, 1)$ so that for any $c_2 \in (0, c_2^0)$ the associated bi-symmetric four rarefaction wave interactions have continuous global solutions, whose centers are vacuum.*

We then take all of c_2^0 under which there exists a global continuous solution regardless of the sign of β on curve bd , and denote the supremum of such c_2^0 by c_2^* , to obtain the main theorem stated in the Introduction.

References

1. Bang, S.: Interaction of three and four rarefaction waves of the pressure-gradient system. *J. Diff. Eqs.* **246**, 453–481 (2009)
2. Bressan, A.: Hyperbolic systems of conservation laws. In: *The One Dimensional Cauchy Problem*. Oxford: Oxford University Press, 2000
3. Chang, T., Chen, G.Q., Yang, S.L.: On the 2-D Riemann problem for the compressible Euler equations, I. Interaction of shock waves and rarefaction waves. *Disc. Cont. Dyn. Syst.* **1**, 555–584 (1995)
4. Chang, T., Hsiao, L.: *The Riemann Problem and Interaction of Waves in Gas Dynamics*. Pitman Monographs and Surveys in Pure and Applied Mathematics, **41**, Harlow: Longman Scientific & Technical, 1989
5. Chen, G.-Q., Feldman, M.: *Global solutions of shock reflection by large-angle wedges for potential flow*. Ann. Math (2), to appear, available at <http://pjim.math.berkeley.edu/annals/ta/080510-Chen/080510-Chen-v1.pdf>
6. Chen, X., Zheng, Y.: The interaction of rarefaction waves of the two-dimensional Euler equations. *Indiana Univ. Math. J.* **58**(2009), No. 6 (in press)
7. Courant, R., Friedrichs, K.O.: *Supersonic Flow and Shock Waves*, New York: Interscience Publishers, Inc., 1948
8. Dafermos, C.: *Hyperbolic Conservation Laws in Continuum Physics*. Grundlehren der mathematischen Wissenschaften, Berlin-Hidelberg-NewYork: Springer, 2000
9. Dinu, L.F.: *Multidimensional Wave-Wave Regular Interactions and Genuine Nonlinearity: Some Remarks*. Lecture presented in Loughborough University, UK, 2006-07
10. Glimm, G., Ji, X., Li, J., Li, X., Zhang, P., Zhang, T., Zheng, Y.: Transonic shock formation in a rarefaction Riemann problem for the 2-D compressible Euler equations. *SIAM J. Appl. Math.* **69**, 720–742 (2008)

11. Kurganov, A., Tadmor, E.: Solution of two-dimensional Riemann problems for gas dynamics without Riemann problem solvers. *Num. Meth. Part. Diff. Eqs.* **18**, 584–608 (2002)
12. Lax, P., Liu, X.: Solutions of two-dimensional Riemann problem of gas dynamics by positive schemes. *SIAM J. Sci. Compt.* **19**, 319–340 (1998)
13. LeFloch, P.G.: *Hyperbolic Systems of Conservation Laws, The Theory of Classical and Non-Classical Shock Waves*. Basel: Birkhäuser Verlag, 2002
14. Li, J.: On the two-dimensional gas expansion for compressible Euler equations. *SIAM J. Appl. Math.* **62**, 831–852 (2001)
15. Li, J., Zhang, T., Yang, S.: *The Two-Dimensional Riemann Problem in Gas Dynamics*. Pitman Monographs and Surveys in Pure and Applied Mathematics **98**, Essex: Addison Wesley Longman limited, 1998
16. Li, J., Zhang, T., Zheng, Y.: Simple waves and a characteristic decomposition of the two dimensional compressible Euler equations. *Commun. Math. Phys.* **267**, 1–12 (2006)
17. Li, J., Zheng, Y.: Interaction of rarefaction waves of the two-dimensional self-similar Euler equations. *Arch. Rat. Mech. Anal.* **193**, 623–657 (2009)
18. Li, M., Zheng, Y.: Semi-hyperbolic patches of solutions of the two-dimensional Euler equations. Preprint, available on request
19. Elling, V., Liu, T.P.: Supersonic flow on a solid wedge. *Comm. Pure Appl. Math.* **61**, 1331–1481 (2008)
20. Majda, A.: *Compressible Fluid Flow and Systems of Conservation Laws in Several Space Variables*. Applied Mathematical Sciences **53**. New York: Springer-Verlag, 1984
21. Pogodin, I.A., Suchkov, V.A., Ianenko, N.N.: On the traveling waves of gas dynamic equations. *J. Appl. Math. Mech.* **22**, 256–267 (1958)
22. Schulz-Rinne, C.W.: Classification of the Riemann problem for two-dimensional gas dynamics. *SIAM J. Math. Anal.* **24**, 76–88 (1993)
23. Schulz-Rinne, C.W., Collins, J.P., Glaz, H.M.: Numerical solution of the Riemann problem for two-dimensional gas dynamics. *SIAM J. Sci. Compt.* **4**, 1394–1414 (1993)
24. Serre, D.: Écoulements de fluides parfaits en deux variables indépendantes de type espace. Réflexion d'un choc plan par un dièdre compressif. *Arch. Rat. Mech. Anal.* **132**, 15–36 (1995)
25. Smoller, J.: *Shock Waves and Reaction-Diffusion Equations*. Berlin-Heidelberg-NewYork: Springer, 1983
26. Song, K., Zheng, Y.: Semi-hyperbolic patches of solutions of the pressure gradient system. *Disc. Cont. Dyn. Syst. Series A* **24**, 1365–1380 (2009)
27. Wang, R., Wu, Z.: On mixed initial boundary value problem for quasilinear hyperbolic system of partial differential equations in two independent variables (in Chinese). *Acta Sci. Natur. Jinlin Univ.*, **2**, 459–502, (1963)
28. Zhang, T., Zheng, Y.: Conjecture on the structure of solution of the Riemann problem for two-dimensional gas dynamics systems. *SIAM J. Math. Anal.* **21**, 593–630 (1990)
29. Zhang, T., Zheng, Y.: Axisymmetric solutions of the Euler equations for polytropic gases. *Arch. Rat. Mech. Anal.* **142**, 253–279 (1998)
30. Zheng, Y.: *Systems of Conservation Laws: Two-Dimensional Riemann Problems*. Vol. **38**, PNLDE, Boston: Birkhäuser, 2001
31. Zheng, Y.: Two-dimensional regular shock reflection for the pressure gradient system of conservation laws. *Acta Math. Appl. Sin. Engl. Ser.* **22**, 177–210 (2006)
32. Zheng, Y.: The compressible Euler system in two space dimensions. In: *Series of Cont. Appl. Math. Vol. 13*, (Shanghai Mathematics Summer School, 2007). G. Q. Chen, T.-T. Li, C. Liu (eds.) Singapore: World Scientific/ Higher Ed. Press, 2008
33. Zheng, Y.: Absorption of characteristics by sonic curves of the two-dimensional Euler equations. *Disc. Cont. Dyn. Syst.* **23**, 605–616 (2009)
34. Zheng, Y.: Shock reflection for the Euler system. In: *Hyperbolic Problems Theory, Numerics and Applications* (Proceedings of the Osaka meeting 2004), Vol. **II**. Eds. F. Asakura (Chief), H. Aiso, S. Kawashima, A. Matsumura, S. Nishibata, K. Nishihara; Yokohama: Yokohama Publishers, 2006, pp. 425–432

Communicated by P. Constantin